Dynamic Base Station Sleep Control via Submodular Optimization for Green mmWave Networks

Akihiro Egami, Takayuki Nishio(✉), Masahiro Morikura, and Koji Yamamoto

Graduate School of Informatics, Kyoto University, Yoshida-honmachi, Sakyo-ku, Kyoto 606-8501, Japan
nishio@i.kyoto-u.ac.jp

Abstract. This paper proposes a dynamic millimeter-wave (mmWave) base station (BS) sleep control scheme for green mmWave networks. The typical coverage radius of mmWave BS is short due to high propagation and shadowing loss, thus large number of BSs are required to be deployed densely. A network consisting of many BSs consumes large energy. Sleep and activation control is a promising technique to reduce energy consumption. However, to select a set of BSs to sleep from large number of BSs to maximize total throughput under on condition that the total energy consumption of the network is limited is a NP-hard problem and it requires huge computation time. This paper formulates sleep control based on submodular optimization which can be solved quickly by using a greedy algorithm and the performance in the worst case is guaranteed to be $(1 - e^{-1})$-approximation. We design a utility function defined as total expected rate for mmWave access networks in consideration of the characteristics of mmWave communication, and prove that it is submodular and monotone. The sleep and activation control of mmWave BSs is formulated as a combinatorial optimization problem to maximize a monotone submodular function under the constraint that the number of BSs to be activated is limited due to energy constraints. Simulation results confirmed that the proposed scheme obtains a BS set achieving higher throughput than random selection and the scheme is polynomial time algorithm.

Keywords: mmWave · Sleep control · Submodular optimization

1 Introduction

The rapidly increasing mobile traffic in mobile access networks, such as cellular networks and wireless local area networks (WLANs), is leading to bandwidth shortages. The millimeter wave (mmWave) band is generally considered a key enabler of both high-speed and high-capacity wireless access for next generation (5G) cellular networks and WLANs [1,2]. Networks operating at this band have

P. Marques et al. (Eds.): CROWNCOM 2017, LNICST 228, pp. 63–74, 2018.
https://doi.org/10.1007/978-3-319-76207-4_6

the ability to provide high-speed and high-capacity wireless Internet access [3,4] because its wide bandwidth enables multi-gigabit per second data transmission rates. However, the coverage of a mmWave base station (BS) is much smaller than that of a conventional BS that uses microwave because of its higher signal propagation loss. Furthermore, the received signal strengths of mmWave communication can be severely degraded when pedestrians block the line-of-sight (LOS) paths [5]. This phenomenon is known as the human blockage problem. In order to provide LOS paths to several users, the dense deployment of a large number of mmWave BSs have to be densely deployed.

However, dense deployment of mmWave BSs consumes a large amount of energy. Energy consumption is also an open issue in microwave communication systems that employ small-cell architectures. To reduce energy consumption, a dynamic BS sleep control scheme is proposed [6,7]. This scheme allows both the redundant BSs to sleep and the other BSs to be activated. The BS activation problem that selects the optimal set of BSs to activate is typically formulated as a combinatorial optimization problem or a non-linear optimization problem, and such problems are typically nondeterministic polynomial time (NP)-hard. Thus, it takes very long time to solve the problem especially when the number of BSs is large. Therefore, an algorithm is needed that can obtain either an optimal or a suboptimal solution in a practical computation time is needed.

Abbasi and Ghaderi [8] proposed a dynamic BS sleep control system for cellular networks via submodular optimization. Submodular optimization is considered in the literature related to combinatorial optimization problems, which are typically NP-hard problem. For submodular optimization, some algorithms that provide good approximations have been proposed [9,10]. In [8], BS sleep control was formulated as a submodular optimization problem and was solved using a heuristic algorithm based on a greedy algorithm that provides $(1-\mathrm{e}^{-1})$-approximation. However, both the radio propagation characteristic and system design of the microwave communications are quite different from those of our target, namely mmWave communications. For example, serious human blockage does not occur in conventional microwave communications. Dynamic handover schemes have been proposed to solve the human blockage problem [11]. The specific BSs that are active affect the dynamic handover gain, which therefore needs to be considered when selecting which BSs should sleep.

This paper proposes a dynamic BS sleep control scheme via submodular optimization for mmWave communication systems with dynamic BS handovers. We design a utility function by considering both the propagation characteristics of mmWaves and the handover gain, and we prove that the utility function is both submodular and monotone. The BS sleep control system is formulated as a combinatorial optimization problem for maximizing a monotone and submodular function under a knapsack constraint, in which the number of active BSs is limited by energy constraints. Our numerical results confirm both that we can quickly obtain satisfactory approximation solutions for the optimization problem using a greedy algorithm and that the proposed sleep control scheme increases the total throughputs of mmWave networks.

2 System Model

Both the BSs and the user terminals (UTs) are deployed in a two-dimensional area. When m BSs and n UTs are deployed, the sets of the BSs and the UTs are represented as $M = \{1, 2, 3, \ldots, m\}$ and $U = \{1, 2, 3, \ldots, n\}$, respectively. In order to reduce energy consumptions, some BSs are activated while the others sleep. We represent a set of active BSs as a subset of the power set $S \in 2^M$. We assume that the total energy consumed by the network is limited. The energy constraint given by

$$\sum_{j \in S} c_j \leq c_{\text{th}}, \quad (1)$$

where c_j represents the energy consumed by BS j and c_{th} represents the limitation on network energy consumption. The limitation of energy consumption limits the maximum number of activated BSs S.

We assume that m BSs are deployed in a hexagonal arrangement where the coverage of adjacent BSs overlap each other so as eliminate coverage holes. Figure 1 shows an example of the deployment of the BSs and the available PHY rate for LOS communication to UTs located in the area. The BSs use directional antennas that have beamforming in all directions. Thus, a BS covers a circular area, which is called a cell. Each user's PHY rate of each UT located in the cell is determined by their received signal strength indicator (RSSI) according to the IEEE 802.11ad standard [12]. Table 1 shows the correspondences between PHY rates and RSSIs. We represent the received signal strength and PHY rate of a communication between UT i and BS j as p_{ij} and $r(p_{ij})$ respectively. UTs in the cell edge eventually use minimum PHY rate for LOS communications.

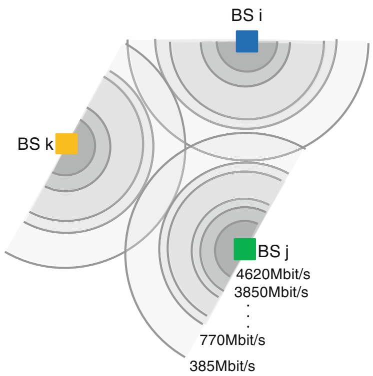

Fig. 1. The deployment of BSs and available rate.

We classify a set of UTs covered by BS j into two subsets of UTs; $R_j, R'_j \subseteq U$. Figure 2 shows an example of R_j, R'_j. UTs in R_j and that in R'_j are covered by only BS j and by multiple BSs including BS j, respectively. For the sake of

Table 1. PHY rates corresponding to RSSIs

PHY rate (Mbit/s)	RSSI (dBm)
385	−68
770	−66
⋮	⋮
3850	−54
4620	−53

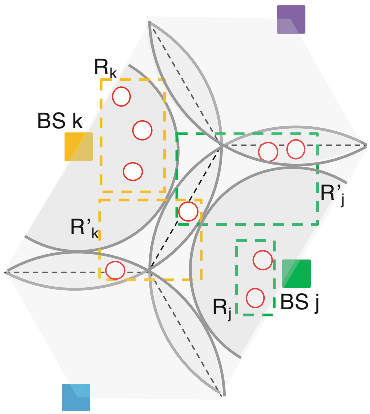

Fig. 2. Subsets of UTs and their locations.

simplicity, this paper assumes that an operator of the system knows R_j and R'_j accurately since UTs can know which BSs cover them from control frames such as beacon transmitted by each BS and the information can be feedbacked to the operator.

Next we mention an assumption for human blockage. As mentioned in Sect. 1, when a pedestrian blocks an LOS path between a BS and a UT, the received signal strength decreases sharpely. The signal attenuation A is modeled as Gaussian distribution with $\mu = 13.4$ and $\sigma = 2.0$ [13]. Thus, PHY rate for NLOS communication becomes $r(p_{ij} - A)$. Moreover, we assume that LOS path blockages occur stochastically, where a link between BS j and UT i is blocked with a certain probability P_{ij} [14].

We explain assumptions for UTs in R'_j. As we mentioned above, since only UTs in the cell edge could be covered by multiple BSs and UTs in the cell edge use minimum PHY rate, UTs in R'_j use minimum PHY rate represented as $r_{\min}$. Since human blockage degrades RSSI 13.4 dB averagely, UTs in R'_j could not communicate with BS j in most case when their links are blocked. Thus, for the sake of simplicity, PHY rate for UTs in R'_j becomes zero when their links are blocked. Furthermore, we assume that a proactive BS handover scheme [15] is activated for UTs covered by multiple BSs. When a LOS path between a UT in R'_j and BS j is blocked, the UT communicating with a BS is transferred to another BS. Thus, the UTs in R'_j can communicate at $r_{\min}$ unless all the links with activated BSs are blocked. When the BSs in set S are activated, the probabilities that all LOS paths for UT i are blocked and that at least one of them is not blocked are, respectively, represented as

$$P_i^{\mathrm{NLOS}}(S) = \prod_{j \in S} P_{ij}^{\mathbb{1}_{R'_j}(i)}, \tag{2}$$

$$P_i^{\mathrm{LOS}}(S) = 1 - \prod_{j \in S} P_{ij}^{\mathbb{1}_{R'_j}(i)}, \tag{3}$$

where $\mathbb{1}_X(y)$ is an indication function that is 1 if X includes y and 0 otherwise.

We assume file download as an application for mmWave access networks. Since mmWave communication could achieve higher throughput than Internet and data server often limit the maximum transmission rate to reduce server load, we assume that the maximum throughput of the download is limited to several tens Mbit/s at the server side.

3 Submodular Optimization for mmWave BS Sleep Control

3.1 Problem Formulation

We consider a BS sleep control problem under the energy constraint (1). We propose a utility function given by

$$G(S) = \sum_{i \in U} \mathbb{E}[r_i], \tag{4}$$

where $\mathbb{E}[r_i]$ is the expected PHY rate of UT i, which is a function of S. $\mathbb{E}[r_i]$ is given as follows:

$$\mathbb{E}[r_i] = \sum_{j \in S} \{(1 - P_{ij})r(p_{ij}) + P_{ij} r(p_{ij} - A)\} \mathbb{1}_{R_j}(i) + r_{\min}\left(1 - \prod_{j \in S} P_{ij}^{\mathbb{1}_{R'_j}(i)}\right). \tag{5}$$

The first and second terms represent average PHY rates for UT i when the UT is covered by a BS and when the UT is covered by multiple BSs. As mentioned in Sect. 2, UTs covered by multiple BSs use minimum PHY rate $r_{\min}$, the rate becomes zero when their links are blocked, and the BS handover could be operated when blockage. Unless all the links are blocked, UTs can communicate with $r_{\min}$, the probability of which is (3).

Maximizing the proposed function increases the average throughput of mmWave communication. Since the capacity of mmWave communication is much larger than those of both conventional WLANs and cellular networks, connecting several users to a BS is preferable so that the capacity of mmWave communication is fully utilized. This is why we employ a summation for the function.

A constraint is the limitation of energy consumption shown in (1). Thus, from (1) and (4), the mmWave BS sleep control problem is formulated as follows:

$$\begin{aligned} &\underset{\boldsymbol{S}}{\text{maximize}} \quad G(S), \\ &\text{subject to} \quad \sum_{j \in S} c_j \leq c_{\text{th}}, \end{aligned} \tag{6}$$

We prove that the objective function increases monotonically and is a submodular function. Before this proof, we introduce both a lemma and a definition, as follows:

Lemma 1. *Let X and Y be sets with $X \cap Y = \emptyset$. Then,*

$$\prod_{j \in X \cup Y} P_{ij}^{\mathbb{1}_{R'_j}(i)} = \prod_{j \in X} P_{ij}^{\mathbb{1}_{R'_j}(i)} \prod_{j \in Y} P_{ij}^{\mathbb{1}_{R'_j}(i)}. \tag{7}$$

Proof. Let $X = \{x_1, x_2, \cdots, x_n\}$ and $Y = \{y_1, y_2, \cdots, y_m | y_i \neq x_j$ for any i and $j\}$, thus $X \cup Y = \{x_1, x_2, \cdots, x_n, y_1, y_2, \cdots, y_m\}$. Therefore,

$$\begin{aligned} \prod_{j \in X \cup Y} P_{ij}^{\mathbb{1}_{R'_j}(i)} &= P_{i,x_1}^{\mathbb{1}_{R'_{x_1}}(i)} \cdots P_{i,x_n}^{\mathbb{1}_{R'_{x_n}}(i)} P_{i,y_1}^{\mathbb{1}_{R'_{y_1}}(i)} P_{i,y_m}^{\mathbb{1}_{R'_{y_m}}(i)} \\ &= \prod_{j \in X} P_{ij}^{\mathbb{1}_{R'_j}(i)} \prod_{j \in Y} P_{ij}^{\mathbb{1}_{R'_j}(i)}. \end{aligned} \tag{8}$$

□

Definition 1. *If $f(S') \leq f(S)$ stands for every $S, S' \in 2^M$ with $S' \subseteq S, f(\cdot)$ is a monotone function.*

Theorem 1. *$G(S)$ is a monotone function.*

Proof. Let $S, S' \in 2^M$ and $S' \subseteq S$

$$\begin{aligned} &G(S) - G(S') \\ &= \sum_{i \in U} \left\{ \sum_{j \in S} \left[(1 - P_{ij}) r(p_{ij}) + P_{ij} r(p_{ij} - A)\right] \mathbb{1}_{R_j}(i) + r_{\min} \left(1 - \prod_{j \in S} P_{ij}^{\mathbb{1}_{R'_j}(i)} \right) \right\} \\ &\quad - \sum_{i \in U} \left\{ \sum_{j \in S'} \left[(1 - P_{ij}) r(p_{ij}) + P_{ij} r(p_{ij} - A)\right] \mathbb{1}_{R_j}(i) + r_{\min} \left(1 - \prod_{j \in S'} P_{ij}^{\mathbb{1}_{R'_j}(i)} \right) \right\} \\ &= \sum_{i \in U} \left\{ \sum_{j \in S \setminus S'} \left[(1 - P_{ij}) r(p_{ij}) + P_{ij} r(p_{ij} - A)\right] \mathbb{1}_{R_j}(i) \right. \\ &\qquad \left. + r_{\min} \prod_{j \in S'} P_{ij}^{\mathbb{1}_{R'_j}(i)} - r_{\min} \prod_{j \in S} P_{ij}^{\mathbb{1}_{R'_j}(i)} \right\}. \end{aligned} \tag{9}$$

Then, Lemma 1 gives

$$(9) = \sum_{i\in U}\left\{\sum_{j\in S\setminus S'}[(1-P_{ij})r(p_{ij})+P_{ij}r(p_{ij}-A)]\mathbb{1}_{R_j}(i) + r_{\min}\left[\prod_{j\in S'}P_{ij}^{\mathbb{1}_{R'_j}(i)}(1-\prod_{j\in S\setminus S'}P_{ij}^{\mathbb{1}_{R'_j}(i)})\right]\right\}. \tag{10}$$

From $P_{ij}\le 1, 0\le r(\cdot)$ and $0<r_{\min}$, (10) ≥ 0. Thus, $G(S')\le G(S)$. □

Now, we prove that the objective function $G(S)$ is a submodular function.

Definition 2. *If, for every $S, S'\in 2^M$ with $S'\subseteq S$, and $x\in 2^M\setminus S$, $f(S\cup x)-f(S)\le f(S'\cup x)-f(S')$ holds, $f(S)$ is a submodular function.*

Theorem 2. *$G(S)$ is a submodular function.*

Proof. Lemma 1 gives

$$\begin{aligned}
&G(S'\cup x)-G(S')-\{G(S\cup x)-G(S)\}\\
&=\sum_{i\in U}\left\{\sum_{j\in x}[(1-P_{ij})r(p_{ij})+P_{ij}r(p_{ij}-A)]\,\mathbb{1}_{R_j}(i)\right.\\
&\qquad\left.+r_{\min}\left[\prod_{j\in S'}P_{ij}^{\mathbb{1}_{R'_j}(i)}\left(1-\prod_{j\in x}P_{ij}^{\mathbb{1}_{R'_j}(i)}\right)\right]\right\}\\
&-\sum_{i\in U}\left\{\sum_{j\in x}[(1-P_{ij})r(p_{ij})+P_{ij}r(p_{ij}-A)]\,\mathbb{1}_{R_j}(i)\right.\\
&\qquad\left.+r_{\min}\left[\prod_{j\in S}P_{ij}^{\mathbb{1}_{R'_j}(i)}\left(1-\prod_{j\in x}P_{ij}^{\mathbb{1}_{R'_j}(i)}\right)\right]\right\}\\
&=\sum_{i\in U}\left[r_{\min}\prod_{j\in S'}P_{ij}^{\mathbb{1}_{R'_j}(i)}\left(1-\prod_{j\in S\setminus S'}P_{ij}^{\mathbb{1}_{R'_j}(i)}\right)\left(1-\prod_{j\in x}P_{ij}^{\mathbb{1}_{R'_j}(i)}\right)\right].
\end{aligned}\tag{11}$$

From $P_{ij}\le 1$ and $0<r_{\min}$, (11) ≥ 0. Thus, $G(S\cup x)-G(S)\le G(S'\cup x)-G(S')$. □

3.2 Algorithms to Solve the Problem

The above-mentioned problem is NP-hard. We employ a greedy algorithm to obtain a solution, which is proved to provide a good approximate solution for submodular optimization. A simple greedy algorithm starts with the empty set

S_0 and, during iteration k, the element maximizing the discrete derivative is added as long as a following constraint is satisfied.

$$S_k = S_{k-1} \cup \{\arg\max_x f(S_{k-1} \cup x) - f(S_{k-1})\}, \tag{12}$$

where $f(\cdot)$ is a monotone and submodular function. Nemhauser et al. [16] proved that a simple greedy algorithm provides a $(1 - \mathrm{e}^{-1})$-approximation for a special case of the problem in which the same $c_j = c$ for all $j \in M$. In our problem, when all BSs consume the same amount of energy, we can employ the greedy algorithm to solve the problem and the solution is guaranteed to provide a $(1 - \mathrm{e}^{-1})$-approximation.

Sviridenko [9] proposed a modified greedy algorithm for problems involving nonnegative integer weights. In iteration k, the modified algorithm selects an element based on the following update rule:

$$S_k = S_{k-1} \cup \{\arg\max_x \frac{f(S_{k-1} \cup x) - f(S_{k-1})}{c_x}\}. \tag{13}$$

Sviridenko proved that the algorithm provides a $(1 - \mathrm{e}^{-1})$-approximation. We could employ this algorithm to solve our problem in a case where each BS consume different amount of energy.

4 Numerical Evaluation

4.1 Simulation Scenario

Figure 3(a) and (b) show examples of the BSs and UTs deployment. We assumed both that n UTs were located in a $300\,\mathrm{m}^2$ area and that they followed two types of distribution.

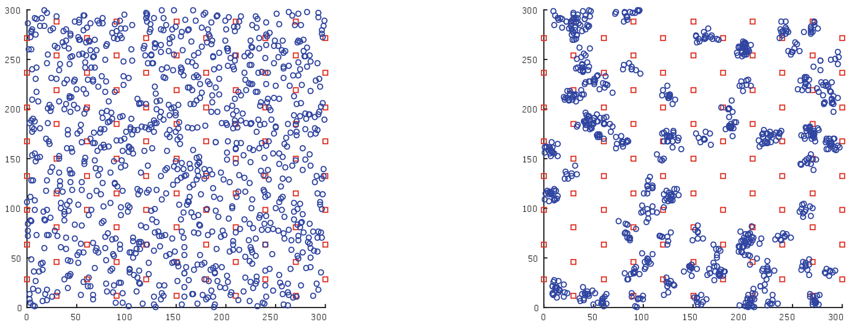

(a) Random distribution (b) Cluster distribution

Fig. 3. Distribution of both BSs (red squares) and UTs (blue circles). (Color figure online)

Random distribution. UTs were located randomly.

Cluster distribution. We assumed that the users in an exhibition hall used a mmWave WLAN. The UTs were distributed based on Matern cluster process, as users might typically be found in such a venue when gathering around displays. In the Matern cluster process, the UTs were deployed for clustering and the locations of the cluster centers were determined according to a Poisson process with an intensity of λ_0. Cluster points were located within a disc of radius R around the centers of the clusters, and the UTs were distributed according to a Poisson process with an intensity of λ_1.

The transmit power and antenna gain for all BSs were set to 20 dBm and 16 dBi, respectively, and the attenuation constant was set to 2. $P_{i,j}$ was set to 0.2 for every value of i and j. The energy cost of activated BS c_j was set to the same value c_{BS} for every BS j. The maximum number of activated BSs was limited to $m_{\mathrm{act}} = c_{\mathrm{th}}/c_{\mathrm{BS}}$, and the constraint (1) was represented as $|S| \leq m_{\mathrm{act}}$.

As mentioned in Sect. 3.1, increasing the sum of the expected PHY rate leads to an increase in the average throughput for mmWave communication. We evaluated the throughput of each activated BS based on the number of packets transmitted successfully while considering both the traffic model and human blockage model. We assumed file download as an application for mmWave access networks, and we assumed that each user accounted for 30 Mbit/s user datagram protocol downlink traffic. We assumed that each user downloaded the file (100 MB) and waited 10 s before starting to download the next one.

We assumed both that the occurrence of human blockage followed the Poisson process and that its interval followed the exponential distribution. t_{b} and t_{nb} represent the duration of human blockage and its interval, respectively, and A represents attenuation. We simplified Ref. [13] for a binary model and then determined the values of both t_{b} and A. t_{b} [s] and A [dB] are according to Weibull distribution ($\lambda = 0.59, k = 6.32$) and Gaussian distribution ($\mu = 13.4, \sigma = 2.0$), respectively. We set the value of t_{nb} such that the ratio of the duration of human blockage duration to the total time was $P_{ij}(= 0.2)$. t_{nb} [s] is according to Exponential distribution ($\lambda = 0.46$).

We evaluated the computational time to solve the sleep control problem, the utility function, defined as the total expected PHY rate, and the total throughput of the activated BSs assuming both file download and human blockage. We compared the proposed scheme with a random selection scheme and a naive scheme. The random selection scheme selected m_{act} BSs randomly. The naive scheme calculated the utilities of all sets of m_{act} BSs and selected the BS set that maximized the utility function.

4.2 Numerical Result

Figure 4 shows computation time of each algorithm as a function of m_{act}. A MacBook Air (13-inch, Mid 2013) was used. The naive scheme with $m_{\mathrm{act}} = 3$ required approximately 134 min to obtain its results, which is too long for

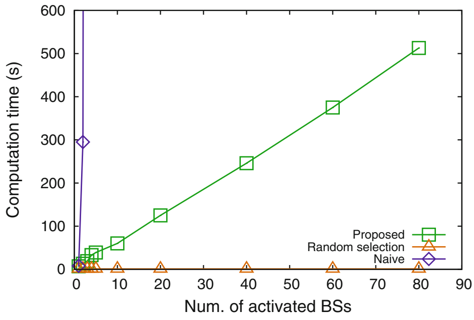

Fig. 4. Computation time vs. m_{act} for $n = 1000$ and $m = 93$.

dynamic sleep control. The time required by the proposed scheme was much shorter than that required by the naive scheme. The computational time for the proposed scheme increased linearly as m_{act} increased. This is because the proposed scheme employing the greedy algorithm calculated the utility function $O(mm_{\text{act}})$ times. The random selection scheme selected a set without calculating the utility function. Hence, its complexity was $O(1)$. The naive scheme calculated the utility function $O(\binom{m}{m_{\text{act}}})$ times.

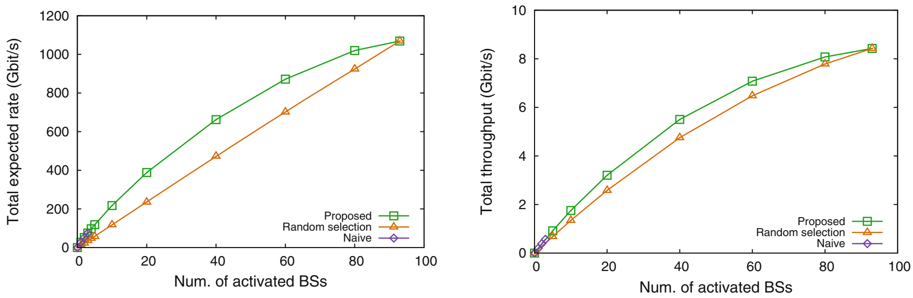

(a) Total expected rate (b) Total throughput

Fig. 5. Total expected rate and total throughput vs. m_{act} for $n = 1000$ and $m = 93$, and randomly distributed UTs.

Random distribution. Figure 5(a) and (b) show the total expected rate and the total throughput as functions of m_{act}, respectively, for when the UTs were distributed randomly. Because the naive scheme took too long to obtain results, we omit them when $m_{\text{act}} \geq 4$. As m_{act} increased, both the total expected rate and total throughput increased because the numbers of UTs covered by the activated BSs increased. The proposed scheme achieved an approximately 40.0% higher total expected rate as well as an approximately 15.8% higher total throughput than the random selection scheme did for $m_{\text{act}} = 40$.

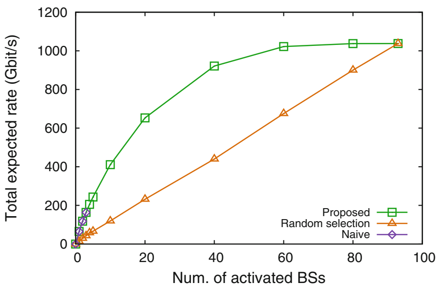

(a) Total expected rate

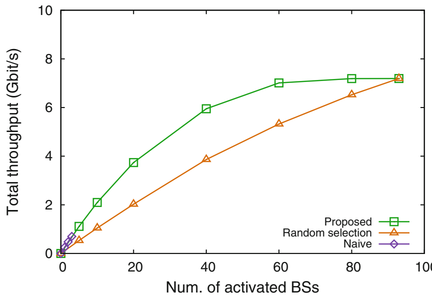

(b) Total throughput

Fig. 6. Total expected rate and total throughput vs. m_{act} for $\lambda_0 = 100/300^2$, $R = 10\,\mathrm{m}$, $\lambda_1 = 900/100\pi R^2$ and $m = 93$, and UTs distributed according to the Matern cluster process.

Cluster distribution. Figure 6(a) and (b) show the total expected rate and the total throughput as functions of m_{act}, respectively, for when the UTs were distributed according to the Matern cluster process. The proposed scheme achieved an approximately 109.3% higher total expected rate as well as an approximately 54.0% higher total throughput than the random selection scheme did for $m_{\mathrm{act}} = 40$. The gain of the proposed scheme was higher than for the case in which UTs were located randomly. Since the UTs were clustered, the number of UTs in each BS varied. Thus, the proposed scheme has the ability to select BSs that increases the throughput, while the random selection scheme might select a BS that has few UTs. As shown in the evaluations, the proposed scheme can obtain a set of BSs to achieve a high throughput with a practical computation time.

5 Conclusion

This paper proposed a dynamic BS sleep control scheme for green mmWave networks. The proposed scheme employed a utility function consisting of both the PHY rate and the probability of LOS path blockage between a BS and a UT. We proved that the proposed utility function both increases monotonically and is submodular. The BS sleep control system is formulated as a submodular optimization problem of maximizing a monotone, submodular function under the knapsack constraint, in which the number of activated BSs was limited due to energy constraints, where a greedy algorithm provided a $(1-\mathrm{e}^{-1})$-approximation for the worst case. The numerical results confirmed both that the proposed scheme could quickly obtain a good approximation for the solution and that maximizing the proposed the objective function increased the average throughput of mmWave communications.

Acknowledgement. This work was supported in part by JSPS KAKENHI Grant Number 17H03266.

References

1. Rappaport, T.S., Sun, S., Mayzus, R., Zhao, H., Azar, Y., Wang, K., Wong, G.N., Schulz, J.K., Samimi, M., Gutierrez, F.: Millimeter wave mobile communications for 5G cellular: it will work!. IEEE Access **1**, 335–349 (2013)
2. Dehos, C., González, J.L., De Domenico, A., Kténas, D., Dussopt, L.: Millimeter-wave access and backhauling: the solution to the exponential data traffic increase in 5G mobile communications systems? IEEE Commun. Mag. **52**(9), 88–95 (2014)
3. Yong, S.K., Chong, C.C.: An overview of multigigabit wireless through millimeter wave technology: potentials and technical challenges. EURASIP J. Wirel. Commun. Netw. **2007**(1), 1–10 (2006)
4. Guo, N., Qiu, R.C., Mo, S.S., Takahashi, K.: 60-GHz millimeter-wave radio: principle, technology, and new results. EURASIP J. Wirel. Commun. Netw. **2007**(1), 48 (2007)
5. Giannetti, F., Luise, M., Reggiannini, R.: Mobile and personal communications in the 60 GHz band: a survey. Wirel. Pers. Commun. **10**(2), 207–243 (1999)
6. Zhou, S., Gong, J., Yang, Z., Niu, Z., Yang, P.: Green mobile access network with dynamic base station energy saving. In: Proceedings of the ACM MobiCom, Beijing, China, vol. 9, no. 262, pp. 10–12, September 2009
7. Oh, E., Krishnamachari, B., Liu, X., Niu, Z.: Toward dynamic energy-efficient operation of cellular network infrastructure. IEEE Commun. Mag. **49**(6), 56–61 (2011)
8. Abbasi, A., Ghaderi, M.: Energy cost reduction in cellular networks through dynamic base station activation. In: Proceedings of the IEEE SECON, Singapore, pp. 363–371 (2014)
9. Sviridenko, M.: A note on maximizing a submodular set function subject to a knapsack constraint. Oper. Res. Lett. **32**(1), 41–43 (2004)
10. Krause, A., Guestrin, C.: Submodularity and its applications in optimized information gathering. ACM Trans. Intell. Syst. Technol. **2**(4), 32 (2011)
11. Oguma, Y., Nishio, T., Yamamoto, K., Morikura, M.: Proactive handover based on human blockage prediction using RGB-D cameras for mmwave communications. IEICE Trans. Commun. **99**(8), 1734–1744 (2016)
12. IEEE Std 802.11ad: Wireless LAN medium access control (MAC) and physical layer (PHY) specifications Amendment 3: Enhancements for Very High Throughput in the 60 GHz Band (2014)
13. Maltsev, A., Erceg, V., Perahia, E., Hansen, C., Maslennikov, R., Lomayev, A., Sevastyanov, A., Khoryaev, A.: Channel models for 60 GHz WLAN systems, Document IEEE 802.11-09/0334r8, May 2010
14. Bai, T., Vaze, R., Heath, R.W.: Analysis of blockage effects on urban cellular networks. IEEE Trans. Wirel. Commun. **13**(9), 5070–5083 (2014)
15. Oguma, Y., Arai, R., Nishio, T., Yamamoto, K., Morikura, M.: Proactive base station selection based on human blockage prediction using RGB-D cameras for mmwave communications. In: Proceedings of IEEE Globecom, San Diego, CA, pp. 1–6, December 2015
16. Nemhauser, G.L., Wolsey, L.A., Fisher, M.L.: An analysis of approximations for maximizing submodular set functions - I. Math. Prog. **14**(1), 265–294 (1978)